ЖЭТФ, 2014, том 146, вып. 3 (9), стр. 631–644

KINEMATIC SPIN-FLUCTUATION MECHANISM OF HIGH-TEMPERATURE SUPERCONDUCTIVITY

N. M. Plakida [a*], ***V. S. Oudovenko*** [b]

[a] *Joint Institute for Nuclear Research*
141980, Dubna, Moscow Region, Russia

[b] *Rutgers University*
08854, New Jersey, USA

Received February 20, 2014

We study d-wave superconductivity in the extended Hubbard model in the strong correlation limit for a large intersite Coulomb repulsion V. We argue that in the Mott–Hubbard regime with two Hubbard subbands, there emerges a new energy scale for the spin-fluctuation coupling of electrons of the order of the electronic kinetic energy W much larger than the exchange energy J. This coupling is induced by the kinematic interaction for the Hubbard operators, which results in the kinematic spin-fluctuation pairing mechanism for $V \lesssim W$. The theory is based on the Mori projection technique in the equation of motion method for the Green's functions in terms of the Hubbard operators. The doping dependence of the superconductivity temperature T_c is calculated for various values of U and V.

DOI: 10.7868/S0044451014090235

1. INTRODUCTION

One of crucial issues in the superconductivity theory is to disclose the mechanism of high-temperature superconductivity (HTSC) in cuprates (see, e. g., [1, 2]). In early studies of the problem, a model of strongly correlated electrons was proposed by Anderson [3], where superconductivity occurs at finite doping in the resonating valence bond state due to the antiferromagnetic (AF) superexchange interaction J. However, the intersite Coulomb interaction (CI) V that in cuprates is of the order of J may destroy the resonating valence bond state and superconducting pairing. Recently, a competition of the intersite CI V and pairing induced by the on-site CI U in the Hubbard model [4] or by the intersite CI V was actively discussed. In particular, it was stressed in [5] that a contribution from the repulsive well-screened weak CI in the first order strongly suppresses the pairing induced by contributions of higher orders, and a possibility of superconductivity "from repulsion" was questioned. Using the renormalization group method, the extended Hubbard model with CI V was studied in [6], where superconducting pairing of various symmetries, extended s-, p-, and d-wave types was found depending on the electron concentration and V. Following the original idea of Kohn–Luttinger [7], it was shown in [8] that the p-wave superconductivity exists in the electronic gas at low density with a strong repulsion U and a relatively strong intersite CI V (also see [9] and the references therein). Studies of the phase diagram within the extended Hubbard model in the weak correlation limit have shown that superconducting pairing of different types of symmetry, s, p, d_{xy}, and $d_{x^2-y^2}$, can occur depending on the CI between the nearest V_1 and the next V_2 neighbor sites and electron hopping parameters between distant sites in a broad region of electron concentration [10].

However, the Fermi-liquid model was considered in the weak correlation limit $U \lesssim W$ in these investigations, while cuprates are Mott–Hubbard (more accurately, charge-transfer) doped insulators, where a theory of strongly correlated electronic systems should be applied for $U \gtrsim W$. Here, $W \sim 4t$ is the electronic kinetic energy for the two-dimensional Hubbard model with the nearest-neighbor hopping parameter t. In the limit of strong correlations, various numerical methods for finite clusters are commonly used. There are many investigations of the conventional Hubbard model (see, e. g., [11–14]), but only a few studies of the extended Hubbard model in which the intersite CI V is taken

*E-mail: plakida@theor.jinr.ru

into account. In particular, in Refs. [15–17], the extended Hubbard model was considered in a broad region of U and V. The results in Refs. [15, 16] show that a strong on-site repulsion U effectively enhances the d-wave pairing, which is preserved for large values of $V \gg J$. In Ref. [17], using the slave-boson representation, it was found that superconductivity is destroyed at a small value of $V = J$. We discuss these results in more detail in Sec. 4.3 by comparing them with our findings.

In our recent paper [18], we studied the extended Hubbard model in the limit of strong correlations by taking the CI V and electron–phonon coupling into account. It was found that the high-T_c d-wave pairing is mediated by the strong kinematic interaction of electrons with spin fluctuations. Contributions coming from a weak CI V and phonons turned out to be small since only $l = 2$ harmonics of the interactions make a contribution to the d-wave pairing.

In this paper, we consider superconductivity in the two-dimensional extended Hubbard model with a large intersite Coulomb repulsion V in the limit of strong correlations to elucidate the spin-fluctuation mechanism of high-temperature superconductivity. We argue that in the two-subband regime for the Hubbard model with $U \gtrsim 6t$, a spin–electron kinematic interaction results from complicated commutation relations for the Hubbard operators (HOs) [19]. This interaction leads to the weak exchange interaction $J = 4t^2/U$ due to interband hopping, and at the same time intraband hopping results in a much stronger kinematic interaction $g_{sf} \sim W \gg J$ of electrons with spin excitations. Therefore, the exchange interaction J is not so important for the spin-fluctuation pairing driven by the strong kinematic interaction g_{sf}. We calculate the doping dependence of the superconducting T_c for various values of U and V and show that as long as V does not exceed the kinematic interaction, $V \lesssim W$, the d-wave pairing is preserved. In calculations, we use the Mori-type projection technique [20] in the equation-of-motion method for thermodynamic Green's functions (GFs) [21] expressed in terms of the HOs. The self-energy in the Dyson equation is calculated in the self-consistent Born approximation (SCBA) as in our previous publications [18, 22].

In Sec. 2, the two-subband extended Hubbard model is introduced and equations for the GFs in the Nambu representation are derived. A self-consistent system of equations for GFs and the self-energy is formulated in Sec. 3. Results and discussion are presented in Sec. 4. Concluding remarks are given in Sec. 5.

2. GENERAL FORMULATION

2.1. Extended Hubbard model

We consider the extended Hubbard model on a square lattice,

$$H = \sum_{i \neq j,\sigma} t_{ij} a^\dagger_{i\sigma} a_{j\sigma} - \mu \sum_i N_i + \\ + \frac{U}{2} \sum_i N_{i\sigma} N_{i\bar{\sigma}} + \frac{1}{2} \sum_{i \neq j} V_{ij}\, N_i N_j, \quad (1)$$

where $t_{i,j}$ are the single-electron hopping parameters, $a^\dagger_{i\sigma}$ and $a_{i\sigma}$ are the Fermi creation and annihilation operators for electrons with spin $\sigma/2$ ($\sigma = \pm 1 = (\uparrow, \downarrow)$, $\bar{\sigma} = -\sigma$) on the lattice site i, U is the on-site CI, and the V_{ij} is the intersite CI. Furthermore, $N_i = \sum_\sigma N_{i\sigma}$, $N_{i\sigma} = a^\dagger_{i\sigma} a_{i\sigma}$ is the number operator and μ is the chemical potential.

In the strong correlation limit, the model describes the Mott–Hubbard insulating state at half-filling ($n = \langle N_i \rangle = 1$) when the conduction band splits into two Hubbard subbands. In this case, the Fermi operators $a^\dagger_{i\sigma}$ and $a_{i\sigma}$ in (1) fail to describe single-particle electron excitations in the system and the Fermi-liquid picture becomes inapplicable to cuprates. The projected-type operators, the HOs, referring to the two subbands, singly occuped $a^\dagger_{i\sigma}(1 - N_{i\bar{\sigma}})$ and doubly occupied $a^\dagger_{i\sigma} N_{i\bar{\sigma}}$, must be introduced. In terms of the HOs, model (1) becomes

$$H = \varepsilon_1 \sum_{i,\sigma} X^{\sigma\sigma}_i + \varepsilon_2 \sum_i X^{22}_i + \frac{1}{2} \sum_{i \neq j} V_{ij} N_i N_j + \\ + \sum_{i \neq j,\sigma} t_{ij} \left\{ X^{\sigma 0}_i X^{0\sigma}_j + X^{2\sigma}_i X^{\sigma 2}_j + \right. \\ \left. + \sigma \left(X^{2\bar{\sigma}}_i X^{0\sigma}_j + \text{H.c.} \right) \right\}, \quad (2)$$

where $\varepsilon_1 = -\mu$ is the single-particle energy and $\varepsilon_2 = U - 2\mu$ is the two-particle energy. The matrix HO $X^{\alpha\beta}_i = |i\alpha\rangle\langle i\beta|$ describes transition from the state $|i, \beta\rangle$ to the state $|i, \alpha\rangle$ on a lattice site i taking four possible states for holes into account: an empty state ($\alpha, \beta = 0$), a singly occupied hole state ($\alpha, \beta = \sigma$), and a doubly occupied hole state ($\alpha, \beta = 2$). The number operator and the spin operators are defined in terms of the HOs as

$$N_i = \sum_\sigma X^{\sigma\sigma}_i + 2X^{22}_i, \quad (3)$$

$$S^\sigma_i = X^{\sigma\bar{\sigma}}_i, \quad S^z_i = (\sigma/2)[X^{\sigma\sigma}_i - X^{\bar{\sigma}\bar{\sigma}}_i]. \quad (4)$$

The chemical potential μ is determined from the equation for the average occupation number for holes

$$n = 1 + \delta = \langle N_i \rangle, \tag{5}$$

where $\langle \dots \rangle$ denotes the statistical average with Hamiltonian (2).

The HOs obey the completeness relation $X_i^{00} + + \sum_\sigma X_i^{\sigma\sigma} + X_i^{22} = 1$, which rigorously preserves the constraint that only one quantum state α can be occupied on any lattice site i. The commutation relations for the HOs

$$\left[X_i^{\alpha\beta}, X_j^{\gamma\delta}\right]_\pm = \delta_{ij}\left(\delta_{\beta\gamma} X_i^{\alpha\delta} \pm \delta_{\delta\alpha} X_i^{\gamma\beta}\right), \tag{6}$$

with the upper sign for Fermi-type operators (such as $X_i^{0\sigma}$) and the lower sign for Bose-type operators (such as N_i in (3) or the spin operators in (4)), result in the so-called kinematic interaction. To demonstrate this, we consider the equation of motion for the HO $X_i^{\sigma 2} = a_{i\sigma}^\dagger a_{i\sigma} a_{i\bar{\sigma}}$ in the Heisenberg representation ($\hbar = 1$):

$$i\frac{d}{dt}X_i^{\sigma 2} = [X_i^{\sigma 2}, H] = \left(U - \mu + \sum_l V_{il}\, N_l\right) X_i^{\sigma 2} + + \sum_{l,\sigma'} t_{il}\left(B_{i\sigma\sigma'}^{22} X_l^{\sigma' 2} - \sigma\, B_{i\sigma\sigma'}^{21} X_l^{0\bar{\sigma}'}\right) - - \sum_l t_{il}\, X_i^{02}\left(X_l^{\sigma 0} + \sigma X_l^{2\bar{\sigma}}\right), \tag{7}$$

where $B_{i\sigma\sigma'}^{\eta\zeta}$ are the Bose-type operators

$$B_{i\sigma\sigma'}^{22} = (X_i^{22} + X_i^{\sigma\sigma})\,\delta_{\sigma'\sigma} + X_i^{\sigma\bar{\sigma}}\,\delta_{\sigma'\bar{\sigma}} = = (N_i/2 + \sigma\, S_i^z)\,\delta_{\sigma'\sigma} + S_i^\sigma\,\delta_{\sigma'\bar{\sigma}}, \tag{8}$$

$$B_{i\sigma\sigma'}^{21} = (N_i/2 + \sigma S_i^z)\delta_{\sigma'\sigma} - S_i^\sigma \delta_{\sigma'\bar{\sigma}}. \tag{9}$$

We see that the hopping amplitudes depend on the number operator in (3) and spin operators (4), which results in the kinematic interaction describing effective scattering of electrons on spin and charge fluctuations. In phenomenological models for cuprates, a dynamical coupling of electrons with spin and charge fluctuations is introduced specified by fitting parameters, while the interaction in Eq. (7) is determined by the hopping energy t_{ij} fixed by the electronic dispersion.

2.2. Green's functions

To consider the superconducting pairing in model (2), we introduce the two-time thermodynamic GF [21] expressed in terms of the four-component Nambu operators $\hat{X}_{i\sigma}$ and $\hat{X}_{i\sigma}^\dagger = (X_i^{2\sigma} X_i^{\bar{\sigma}0} X_i^{\bar{\sigma}2} X_i^{0\sigma})$:

$$\mathsf{G}_{ij\sigma}(t - t') = -i\theta(t - t')\langle\{\hat{X}_{i\sigma}(t), \hat{X}_{j\sigma}^\dagger(t')\}\rangle \equiv \equiv \langle\langle \hat{X}_{i\sigma}(t) | \hat{X}_{j\sigma}^\dagger(t')\rangle\rangle, \tag{10}$$

where $\{A, B\} = AB + BA$, $A(t) = e^{iHt} A e^{-iHt}$, and $\theta(x) = 1$ for $x > 0$ and $\theta(x) = 0$ for $x < 0$. The Fourier representation in the $(\mathbf{k}, \omega)$-space is defined by the relations

$$\mathsf{G}_{ij\sigma}(t - t') = \frac{1}{2\pi}\int\limits_{-\infty}^{\infty} dt \exp\left[-i(t - t')\right] \mathsf{G}_{ij\sigma}(\omega), \tag{11}$$

$$\mathsf{G}_{ij\sigma}(\omega) = \frac{1}{N}\sum_{\mathbf{k}} \exp[i\mathbf{k}\cdot(\mathbf{i} - \mathbf{j})]\mathsf{G}_\sigma(\mathbf{k}, \omega). \tag{12}$$

Green's function (12) can be conveniently written in the matrix form

$$\mathsf{G}_\sigma(\mathbf{k}, \omega) = \begin{pmatrix} \hat{G}_\sigma(\mathbf{k}, \omega) & \hat{F}_\sigma(\mathbf{k}, \omega) \\ \hat{F}_\sigma^\dagger(\mathbf{k}, \omega) & -\hat{G}_{\bar{\sigma}}(-\mathbf{k}, -\omega) \end{pmatrix}, \tag{13}$$

where the normal $\hat{G}_\sigma(\mathbf{k}, \omega)$ and anomalous (pair) $\hat{F}_\sigma(\mathbf{k}, \omega)$ GFs are 2×2 matrices for two Hubbard subbands:

$$\hat{G}_\sigma(\mathbf{k}, \omega) = \langle\langle \begin{pmatrix} X_{\mathbf{k}}^{\sigma 2} \\ X_{\mathbf{k}}^{0\bar{\sigma}} \end{pmatrix} | X_{\mathbf{k}}^{2\sigma} X_{\mathbf{k}}^{\bar{\sigma}0}\rangle\rangle_\omega, \tag{14}$$

$$\hat{F}_\sigma(\mathbf{k}, \omega) = \langle\langle \begin{pmatrix} X_{\mathbf{k}}^{\sigma 2} \\ X_{\mathbf{k}}^{0\bar{\sigma}} \end{pmatrix} | X_{-\mathbf{k}}^{\bar{\sigma}2} X_{-\mathbf{k}}^{0\sigma}\rangle\rangle_\omega. \tag{15}$$

To calculate GF (10), we use the equation-of-motion method by differentiating the GF with respect to the times t and t'. As described in detail in Refs. [18, 22], using the Mori-type projection method [20], we derive an exact representation for GF (13) in the form of the Dyson equation

$$\mathsf{G}_\sigma(\mathbf{k}, \omega) = [\omega\tilde{\tau}_0 - \mathsf{E}_\sigma(\mathbf{k}) - \mathsf{Q}\Sigma_\sigma(\mathbf{k}, \omega)]^{-1}\,\mathsf{Q}, \tag{16}$$

where $\tilde{\tau}_0$ is a 4×4 unit matrix. The electron excitation spectrum in the generalized mean-field approximation (GMFA) is determined by the time-independent matrix of correlation functions:

$$\mathsf{E}_\sigma(\mathbf{k}) = \frac{1}{N}\sum_{\mathbf{k}} \exp[i\mathbf{k}\cdot(\mathbf{i} - \mathbf{j})]\langle\{[\hat{X}_{i\sigma}, H], \hat{X}_{j\sigma}^\dagger\}\rangle \mathsf{Q}^{-1} = = \begin{pmatrix} \hat{\varepsilon}(\mathbf{k}) & \hat{\Delta}_\sigma(\mathbf{k}) \\ \hat{\Delta}_\sigma^*(\mathbf{k}) & -\hat{\varepsilon}_{\bar{\sigma}}(\mathbf{k}) \end{pmatrix}, \tag{17}$$

where $\hat{\varepsilon}(\mathbf{k})$ and $\hat{\Delta}_\sigma(\mathbf{k})$ are the normal and anomalous parts of the energy matrix. The parameter $\mathsf{Q} = = \langle\{\hat{X}_{i\sigma}, \hat{X}_{i\sigma}^\dagger\}\rangle = \hat{\tau}_0 \times \hat{Q}$, where $\hat{\tau}_0$ is the unit 2×2 matrix and

$$\hat{Q} = \begin{pmatrix} Q_2 & 0 \\ 0 & Q_1 \end{pmatrix}$$

describes the redistribution of spectral weights with doping the Hubbard subbands

$$Q_2 = \langle X_i^{22} + X_i^{\sigma\sigma}\rangle = n/2, \quad Q_1 = \langle X_i^{00} + X_i^{\bar\sigma\bar\sigma}\rangle = 1 - Q_2.$$

The self-energy operator in Eq. (16),

$$\mathsf{Q}\Sigma_\sigma(\mathbf{k},\omega) = \langle\langle \hat Z^{(ir)}_{\mathbf{k}\sigma} | \hat Z^{(ir)\dagger}_{\mathbf{k}\sigma}\rangle\rangle^{(pp)}_\omega \; \mathsf{Q}^{-1}, \tag{18}$$

is determined by irreducible operators

$$\hat Z^{(ir)}_{i\sigma} = [\hat X_{i\sigma}, H] - \sum_l \mathsf{E}_{il\sigma}\hat X_{l\sigma}$$

and describes processes of inelastic scattering of electrons (holes) on spin and charge fluctuations due to the kinematic interaction and the CI V_{ij} (see Eq. (7)). Self-energy operator (18) can be written in the same matrix form as GF (13):

$$\mathsf{Q}\Sigma_\sigma(\mathbf{k},\omega) = \begin{pmatrix} \hat M_\sigma(\mathbf{k},\omega) & \hat\Phi_\sigma(\mathbf{k},\omega) \\ \hat\Phi^\dagger_\sigma(\mathbf{k},\omega) & -\hat M_{\bar\sigma}(\mathbf{k},-\omega)\end{pmatrix}\mathsf{Q}^{-1}, \tag{19}$$

where the matrices $\hat M$ and $\hat\Phi$ denote the respective normal and anomalous (pair) components of the self-energy operator.

The system of equations for the 4×4 matrix GF (13) and the self-energy (19) can be reduced to a system of equations for $\hat G_\sigma(\mathbf{k},\omega)$ and $\hat F_\sigma(\mathbf{k},\omega)$, the respective normal and pair 2×2 matrix components. Using representations for energy matrix (17) and self-energy (19), we derive the following system of matrix equations for these components:

$$\hat G(\mathbf{k},\omega) = \Big(\hat G_N(\mathbf{k},\omega)^{-1} + \\ + \hat\varphi_\sigma(\mathbf{k},\omega)\,\hat G_N(\mathbf{k},-\omega)\,\hat\varphi^*_\sigma(\mathbf{k},\omega)\Big)^{-1}\hat Q, \tag{20}$$

$$\hat F_\sigma(\mathbf{k},\omega) = -\hat G_N(\mathbf{k},-\omega)\,\hat\varphi_\sigma(\mathbf{k},\omega)\,\hat G(\mathbf{k},\omega), \tag{21}$$

where we introduced the normal-state GF

$$\hat G_N(\mathbf{k},\omega) = \Big(\omega\hat\tau_0 - \hat\varepsilon(\mathbf{k}) - \hat M(\mathbf{k},\omega)/\hat Q\Big)^{-1}, \tag{22}$$

and the superconducting-gap function

$$\hat\varphi_\sigma(\mathbf{k},\omega) = \hat\Delta_\sigma(\mathbf{k}) + \hat\Phi_\sigma(\mathbf{k},\omega)/\hat Q. \tag{23}$$

Dyson equation (16) with the zeroth-order quasiparticle excitation energy (17) and self-energy (19) gives an exact representation for GF (10). To obtain a closed system of equations, the multiparticle GF in self-energy operator (18) should be evaluated as discussed below.

3. APPROXIMATE SYSTEM OF EQUATIONS

In this section, we derive an approximate system of equations for the GFs and the self-energy components in Eqs. (20)–(23) for the two Hubbard subbands by adopting several approximations to make the system of equations numerically tractable.

3.1. Generalized mean-field approximation

Energy matrix (17) is calculated using commutation relations (6) for the HOs. The normal part of the energy matrix $\hat\varepsilon(\mathbf{k})$ after diagonalization determines the quasiparticle spectrum in two Hubbard subbands in the GMFA (see [22] for the details):

$$\varepsilon_{1,2}(\mathbf{k}) = \frac{1}{2}[\omega_2(\mathbf{k}) + \omega_1(\mathbf{k})] \mp \frac{1}{2}\Lambda(\mathbf{k}), \tag{24}$$

$$\omega_\iota(\mathbf{k}) = 4t\,\alpha_\iota\gamma(\mathbf{k}) + 4\,\beta_\iota\,t'\gamma'(\mathbf{k}) + 4\,\beta_\iota\,t''\gamma''(\mathbf{k}) + \\ + \omega^{(c)}_\iota(\mathbf{k}) + U\delta_{\iota,2} - \mu, \quad (\iota = 1,2), \tag{25}$$

where

$$\Lambda(\mathbf{k}) = \{[\omega_2(\mathbf{k}) - \omega_1(\mathbf{k})]^2 + 4W(\mathbf{k})^2\}^{1/2},$$

$$W(\mathbf{k}) = 4t\alpha_{12}\gamma(\mathbf{k}) + 4t'\beta_{12}\gamma'(\mathbf{k}) + 4t''\beta_{12}\gamma''(\mathbf{k}),$$

the hopping parameter is defined by

$$t_{ij} = \frac{1}{N}\sum_{\mathbf{k}} \exp[i\mathbf{k}\cdot(\mathbf{i}-\mathbf{j})]t(\mathbf{k}), \tag{26}$$

$$t(\mathbf{k}) = 4t\gamma(\mathbf{k}) + 4t'\,\gamma'(\mathbf{k}) + 4t''\,\gamma''(\mathbf{k}), \tag{27}$$

the nearest-neighbor hopping is t, the diagonal hopping is t', and the third-neighbor hopping is t''. The corresponding $\mathbf{k}$-dependent functions are

$$\gamma(\mathbf{k}) = (1/2)(\cos k_x + \cos k_y), \quad \gamma'(\mathbf{k}) = \cos k_x \cos k_y,$$

$$\gamma''(\mathbf{k}) = (1/2)(\cos 2k_x + \cos 2k_y)$$

(the lattice constants $a_x = a_y$ are set equal to unity). The contribution from the CI V_{ij} in (25) is given by

$$\omega^{(c)}_{1(2)}(\mathbf{k}) = \frac{1}{N}\sum_{\mathbf{q}} V(\mathbf{k}-\mathbf{q})N_{1(2)}(\mathbf{q}), \tag{28}$$

where $N_1(\mathbf{q}) = \langle X^{0\bar\sigma}_{\mathbf{q}} X^{\bar\sigma 0}_{\mathbf{q}}\rangle/Q_1$ and $N_2(\mathbf{q}) = \langle X^{\sigma 2}_{\mathbf{q}} X^{2\sigma}_{\mathbf{q}}\rangle/Q_2$ are occupation numbers in the respective single-particle and two-particle subbands, and $V(\mathbf{q})$ is the Fourier transform of V_{ij}.

The kinematic interaction for the HOs results in a renormalization of spectrum (24) determined by the parameters

$$\alpha_\iota = Q_\iota \left(1 + \frac{C_1}{Q_\iota^2}\right), \quad \beta_\iota = Q_\iota \left(1 + \frac{C_2}{Q_\iota^2}\right),$$

$$\alpha_{12} = \sqrt{Q_1 Q_2}\left(1 - \frac{C_1}{Q_1 Q_2}\right),$$

$$\beta_{12} = \sqrt{Q_1 Q_2}\left(1 - \frac{C_2}{Q_1 Q_2}\right).$$

In addition to the conventional Hubbard-I renormalization given by the Q_1 and Q_2 parameters, an essential renormalization is caused by the AF spin correlation functions for nearest-neighbors and next neighbors:

$$C_1 = \langle \mathbf{S}_i \mathbf{S}_{i+a_1} \rangle, \quad C_2 = \langle \mathbf{S}_i \mathbf{S}_{i+a_2} \rangle. \tag{29}$$

These functions strongly depend on doping, resulting in a considerable variation of the electronic spectrum, as is shown below and is discussed in detail in Ref. [22].

The anomalous component $\hat{\Delta}_\sigma(\mathbf{k})$ of matrix (17) determines the superconducting gap in the GMFA. The diagonal matrix components in the coordinate representation are given by the equations

$$\Delta_{ij\sigma}^{22} Q_2 = -\sigma t_{ij}^{21} \langle X_i^{02} N_j \rangle - V_{ij} \langle X_i^{\sigma 2} X_j^{\bar{\sigma} 2} \rangle, \tag{30}$$

$$\Delta_{ij\sigma}^{11} Q_1 = \sigma t_{ij}^{12} \langle N_j X_i^{02} \rangle - V_{ij} \langle X_i^{0\bar{\sigma}} X_j^{0\sigma} \rangle, \tag{31}$$

where we introduced upper indexes for the hopping parameter t_{ij}^{12} and t_{ij}^{21} to stress that the anomalous components $\langle X_i^{02} N_j \rangle$ are induced by the interband hopping. Calculating the correlation function $\langle X_i^{02} N_j \rangle$ from the equation of motion for the GF $L_{ij}(t-t') = \langle\langle X_i^{02}(t) | N_j(t') \rangle\rangle$ yields a superconducting gap in the two-particle subband (see Ref. [23] for the details):

$$\Delta_{ij\sigma}^{22} = (J_{ij} - V_{ij}) \langle X_i^{\sigma 2} X_j^{\bar{\sigma} 2} \rangle / Q_2, \tag{32}$$

where $J_{ij} = 4(t_{ij}^{12})^2/U$ is the AF exchange interaction. A similar equation holds for the gap in the single-particle subband:

$$\Delta_{ij\sigma}^{11} = (J_{ij} - V_{ij}) \langle X_i^{0\bar{\sigma}} X_j^{0\sigma} \rangle / Q_1.$$

Therefore, the pairing in the Hubbard model in the GMFA is similar to superconductivity in the t–J model mediated by the AF exchange interaction J_{ij}.

3.2. Self-energy operator

The self-energy matrix (19) due to the kinematic interaction, as shown in Eq. (7), is determined by the multiparticle GFs such as $\langle\langle \hat{X}_{l\sigma'}(t) B_{i\sigma\sigma'}(t) | \hat{X}_{l'\sigma''}^{\dagger} B_{j\sigma\sigma''}^{\dagger} \rangle\rangle$. We calculate the self-energy matrix in the SCBA using the mode-coupling approximation for the multiparticle GFs. In this approximation, the propagation of excitations described by Fermi-like operators $\hat{X}_{l\sigma}$ and Bose-like operators $B_{i\sigma\sigma'}$ for $l \neq i$ is assumed to be independent. Therefore, the corresponding time-dependent multiparticle correlation functions can be written as products of fermionic and bosonic correlation functions,

$$\langle X_{l'}^{2\sigma''} B_{j\sigma\sigma''}^{\dagger} | B_{i\sigma\sigma'}(t) X_l^{\sigma' 2}(t) \rangle = \\ = \delta_{\sigma',\sigma''} \langle X_{l'}^{2\sigma'} X_l^{\sigma' 2}(t) \rangle \langle B_{j\sigma\sigma'}^{\dagger} | B_{i\sigma\sigma'}(t) \rangle, \tag{33}$$

$$\langle X_{l'}^{\bar{\sigma}'' 2} B_{j\bar{\sigma}\bar{\sigma}''} | B_{i\sigma\sigma'}(t) X_l^{\sigma' 2}(t) \rangle = \\ = \delta_{\sigma',\sigma''} \langle X_{l'}^{\bar{\sigma}' 2} X_l^{\sigma' 2}(t) \rangle \langle B_{j\bar{\sigma}\bar{\sigma}'} B_{i\sigma\sigma'}(t) \rangle. \tag{34}$$

The time-dependent single-particle correlation functions are calculated self-consistently using the corresponding GFs. This approximation results in a self-consistent system of equations for self-energy (19) and GFs (20) and (21) similar to the strong-coupling Eliashberg theory [24] (see Ref. [18] and Ch. A in Ref. [2] for the details).

In this approximation, the normal-state GF (22) for two subbands takes the form [22]

$$G_N^{11(22)}(\mathbf{k}, \omega) = [1 - b(\mathbf{k})] G_{1(2)}(\mathbf{k}, \omega) + \\ + b(\mathbf{k}) G_{2(1)}(\mathbf{k}, \omega), \tag{35}$$

$$G_{1(2)}(\mathbf{k}, \omega) = \frac{1}{\omega - \varepsilon_{1(2)}(\mathbf{k}) - \Sigma(\mathbf{k}, \omega)}, \tag{36}$$

with the hybridization parameter $b(\mathbf{k}) = [\varepsilon_2(\mathbf{k}) - \omega_2(\mathbf{k})] / [\varepsilon_2(\mathbf{k}) - \varepsilon_1(\mathbf{k})]$. The self-energy $\Sigma(\mathbf{k}, \omega)$ can be approximated by the same function for two subbands. In the imaginary frequency representation, $i\omega_n = i\pi T(2n+1)$, $n = 0, \pm 1, \pm 2, \ldots$ it is given by

$$\Sigma(\mathbf{k}, \omega_n) = -\frac{T}{N} \sum_{\mathbf{q}} \sum_m \lambda^{(+)}(\mathbf{q}, \mathbf{k}-\mathbf{q} | \omega_n - \omega_m) \times \\ \times [G_1(\mathbf{q}, \omega_m) + G_2(\mathbf{q}, \omega_m)] \equiv \\ \equiv i\omega_n [1 - Z(\mathbf{k}, \omega_n)] + X(\mathbf{k}, \omega_n). \tag{37}$$

The normal GF (36) for the two subbands takes the form

$$\{G_{1(2)}(\mathbf{k},\omega_n)\}^{-1} = i\omega_n - \varepsilon_{1(2)}(\mathbf{k}) - \Sigma(\mathbf{k},\omega_n) = \\ = i\omega_n Z(\mathbf{k},\omega_n) - [\varepsilon_{1(2)}(\mathbf{k}) + X(\mathbf{k},\omega_n)]. \quad (38)$$

To calculate T_c, we can use a linear approximation for the pair GF in (21). In particular, Eq. (23) for the two-particle subband gap $\varphi(\mathbf{k},\omega) = \sigma\varphi_{2,\sigma}(\mathbf{k},\omega)$ can be written as

$$\varphi(\mathbf{k},\omega_n) = \frac{T_c}{N}\sum_{\mathbf{q}}\sum_{m}\{J(\mathbf{k}-\mathbf{q}) - V(\mathbf{k}-\mathbf{q}) + \\ + \lambda^{(-)}(\mathbf{q},\mathbf{k}-\mathbf{q}|\omega_n-\omega_m)\}\times \\ \times \frac{[1-b(\mathbf{q})]^2\,\varphi(\mathbf{q},\omega_m)}{[\omega_m Z(\mathbf{q},\omega_m)]^2 + [\varepsilon_2(\mathbf{q}) + X\mathbf{q},\omega_m)]^2}. \quad (39)$$

The interaction functions in (37) and (39) in the imaginary frequency representation are given by

$$\lambda^{(\pm)}(\mathbf{q},\mathbf{k}-\mathbf{q}|\nu_n) = -|t(\mathbf{q})|^2\,\chi_{sf}(\mathbf{k}-\mathbf{q},\nu_n) \mp \\ \mp\{|V(\mathbf{k}-\mathbf{q})|^2 + |t(\mathbf{q})|^2/4\}\,\chi_{cf}(\mathbf{k}-\mathbf{q},\nu_n). \quad (40)$$

The spectral densities of bosonic excitations are determined by the dynamic susceptibility for spin (sf) and number (charge) (cf) fluctuations

$$\chi_{sf}(\mathbf{q},\omega) = -\langle\langle \mathbf{S}_{\mathbf{q}}|\mathbf{S}_{-\mathbf{q}}\rangle\rangle_\omega, \quad (41)$$
$$\chi_{cf}(\mathbf{q},\omega) = -\langle\langle \delta N_{\mathbf{q}}|\delta N_{-\mathbf{q}}\rangle\rangle_\omega \quad (42)$$

written in terms of the commutator GFs [21] for the spin $\mathbf{S}_{\mathbf{q}}$ and number $\delta N_{\mathbf{q}} = N_{\mathbf{q}} - \langle N_{\mathbf{q}}\rangle$ operators.

Thus, we have derived a self-consistent system of equations for the normal GF (38), self-energy (37), and gap function (39). In the SCBA, vertex corrections to the kinematic interaction $t(\mathbf{q})$ of electrons with spin- and charge-fluctuations (41) and (42) induced by the intraband hopping are neglected. It is assumed that the system is far away from a charge instability or a stripe formation and charge fluctuations give a small contribution to the pairing. The largest contribution from spin fluctuations comes from wave vectors close the AF wave vector $\mathbf{Q} = (\pi,\pi)$, where their energy $\omega_s(\mathbf{Q})$ is much smaller than the Fermi energy, $\omega_s(\mathbf{Q})/\mu \ll 1$ (see, e. g., [25]). Therefore, vertex corrections to the kinematic interaction should be small as in the Eliashberg theory [24] for electron interaction with phonons, where $\omega_{ph}(\mathbf{q})/\mu \ll 1$. Consequently, the SCBA for the self-energy and the GFs calculated self-consistently is quite reliable and allows considering the strong coupling regime, which is essential in the study of renormalization of the quasiparticle spectrum and the superconducting pairing, as shown in Refs. [18, 22] and is discussed below.

4. RESULTS AND DISCUSSION

In numerical computations, we have used models for the CIs and the susceptibility in (41) and (42). For the intersite CI V_{ij}, we consider a model for repulsion of two electrons (holes) on neighboring lattice sites,

$$V(\mathbf{q}) = 2V(\cos q_x + \cos q_y), \quad (43)$$

with the values $V = 0,\ 0.5\,t,\ 1.0t,\ 2.0t$. For the on-site CI, we consider $U = 8t, 16t, 32t$. The AF exchange interaction for neighboring sites is described by the function $J(\mathbf{q}) = 2J(\cos q_x + \cos q_y)$. We note that in the GMFA, the CIs V_{ij} give no contribution to the exchange interaction J_{ij}, and it is therefore assumed to be the same for all values of V (cf. Refs. [15, 16]). In most of the calculations, we take $J = 0.4t$, but to study the role of the spin-fluctuation interaction in the superconducting pairing, we also consider other values of the interaction, $J = 0.2t, 0.6t, 1.0t$.

Due to a large energy scale of charge fluctuations, of the order of several t, in comparison with the spin excitation energy of the order of J, the charge fluctuation contributions can be considered in the static limit for susceptibility (42):

$$\chi_{cf}(\mathbf{k}) = \chi^{(1)}_{cf}(\mathbf{k}) + \chi^{(2)}_{cf}(\mathbf{k}), \\ \chi^{(\alpha)}_{cf}(\mathbf{k}) = -\frac{1}{N}\sum_{\mathbf{q}}\frac{N^{(\alpha)}(\mathbf{q}+\mathbf{k}) - N^{(\alpha)}(\mathbf{q})}{\varepsilon_\alpha(\mathbf{q}+\mathbf{k}) - \varepsilon_\alpha(\mathbf{q})}, \quad (44)$$

where the occupation numbers $N^{(\alpha)}(\mathbf{q})$ are defined as

$$N^{(1)}(\mathbf{k}) = [Q_1 + (n-1)b(\mathbf{k})]\,N_1(\mathbf{k}), \\ N^{(2)}(\mathbf{k}) = [Q_2 - (n-1)b(\mathbf{k})]\,N_2(\mathbf{k}), \\ N_\alpha(\mathbf{k}) = \frac{1}{2} + T\sum_m G_\alpha(\mathbf{k},\omega_m). \quad (45)$$

For the dynamical spin susceptibility $\chi_{sf}(\mathbf{q},\omega)$ in (41), we used a model suggested in Ref. [26]

$$\mathrm{Im}\,\chi_{sf}(\mathbf{q},\omega+i0^+) = \chi_{sf}(\mathbf{q})\chi''_{sf}(\omega) = \\ = \frac{\chi_Q}{1+\xi^2[1+\gamma(\mathbf{q})]}\,\mathrm{th}\,\frac{\omega}{2T}\,\frac{1}{1+(\omega/\omega_s)^2}. \quad (46)$$

This type of the spin-excitation spectrum was found in the microscopic theory for the t–J model in Ref. [25]. The model is determined by two parameters: the AF correlation length ξ and the cut-off energy of spin excitations of the order of the exchange energy $\omega_s \sim J$. The strength of the spin-fluctuation interaction given by the static susceptibility $\chi_Q = \chi_{sf}(\mathbf{Q})$ at the AF wave vector $\mathbf{Q} = (\pi,\pi)$,

$$\chi_Q = \frac{3(1-\delta)}{2\omega_s}\left\{\frac{1}{N}\sum_{\mathbf{q}}\frac{1}{1+\xi^2[1+\gamma(\mathbf{q})]}\right\}^{-1}, \quad (47)$$

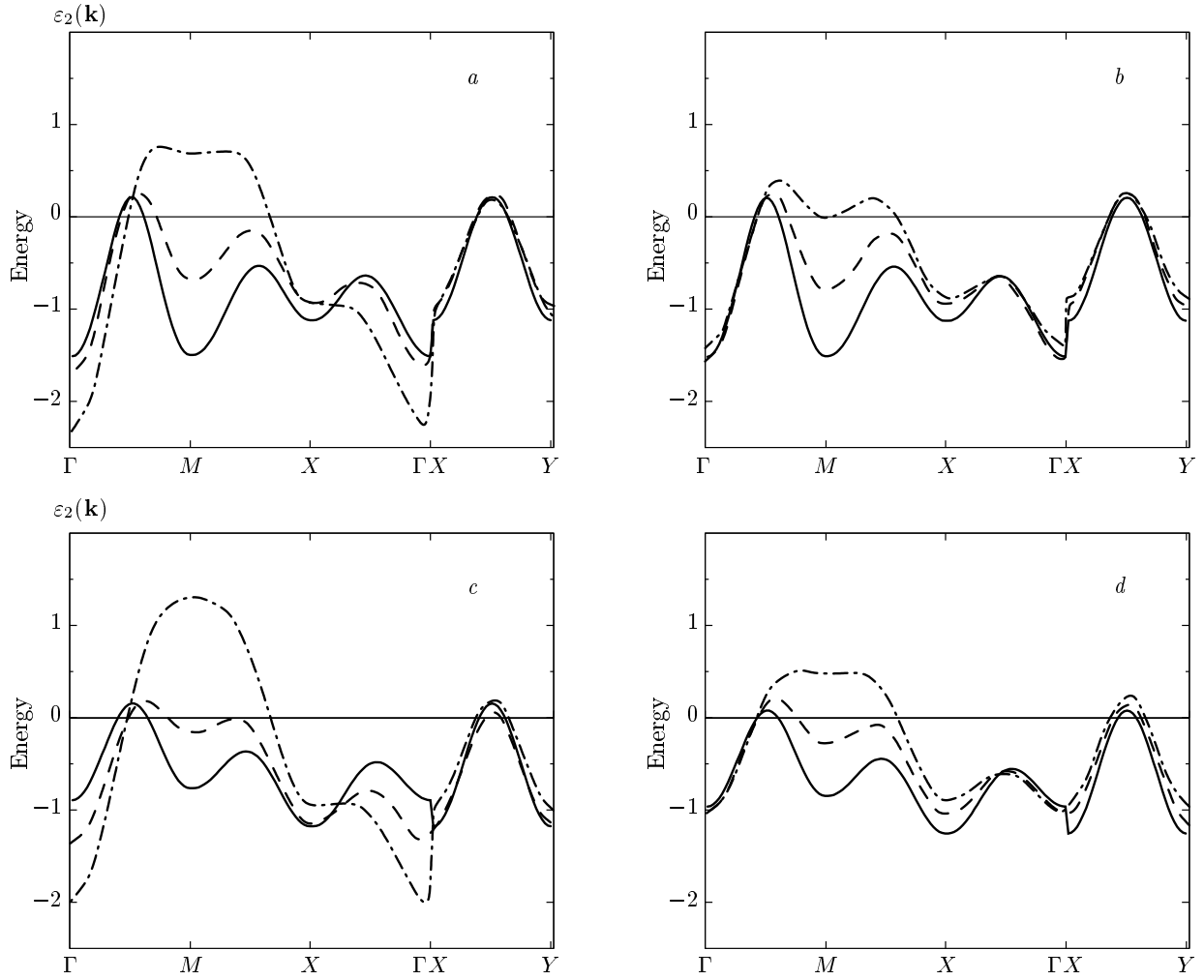

Fig. 1. Electron dispersion $\varepsilon_2(\mathbf{k})$ in the GMFA for (*a* and *c*) $V = 0$ and (*b* and *d*) $V = 2$ at (*a* and *b*) $U = 8$ and (*c* and *d*) $U = 16$ along the symmetry directions $\Gamma(0,0) \to M(\pi,\pi) \to X(\pi,0) \to \Gamma(0,0)$ and $X(\pi,0) \to Y(0,\pi)$ for $\delta = 0.05$ (solid line), $\delta = 0.10$ (dashed line), and $\delta = 0.25$ (dash-dotted line). The Fermi energy for hole doping is at $\omega = 0$

is defined by the normalization condition

$$\frac{1}{N}\sum_{\mathbf{q}}\int_0^\infty \frac{d\omega}{\pi}\,\mathrm{ch}\,\frac{\omega}{2T}\,\mathrm{Im}\,\chi_{sf}(\mathbf{q},\omega) = \langle \mathbf{S}_i^2\rangle = \frac{3}{4}(1-\delta).$$

Spin correlation functions (29) in single-particle excitation spectrum (24) are calculated using the same model (46):

$$C_1 = \frac{1}{N}\sum_{\mathbf{q}} C_{\mathbf{q}}\gamma(\mathbf{q}), \quad C_2 = \frac{1}{N}\sum_{\mathbf{q}} C_{\mathbf{q}}\,\gamma'(\mathbf{q}),$$

where

$$C_{\mathbf{q}} = \frac{\omega_s}{2}\frac{\chi_Q}{1+\xi^2[1+\gamma(\mathbf{q})}.$$

We use $t = 0.4$ eV as an energy unit, and take $t' = -0.2t$ and $t'' = 0.1t$ for the hopping parameters. Below, we present numerical results for the hole-doped case of the two-hole subband.

4.1. Electronic spectrum in the normal state

We first consider the results in the GMFA for electronic spectrum (24). The doping dependence of the electron dispersion for the two-hole subband $\varepsilon_2(\mathbf{k})$ along the symmetry directions in the 2D Brillouin zone (BZ) is shown in Figs. 1*a* and 1*b* for $U = 8$ and in Figs. 1*c* and 1*d* for $U = 16$ for $V = 0$ and for $V = 2$. The corresponding Fermi surfaces determined by the equation $\varepsilon_2(\mathbf{k}_\mathrm{F}) = 0$ are plotted in Fig. 2. For small doping, $\delta = 0.05$, the energies at the $M(\pi,\pi)$ and $\Gamma(0,0)$ points are nearly equal, as in the AF phase. Only small hole-like Fermi-surface pockets close to the

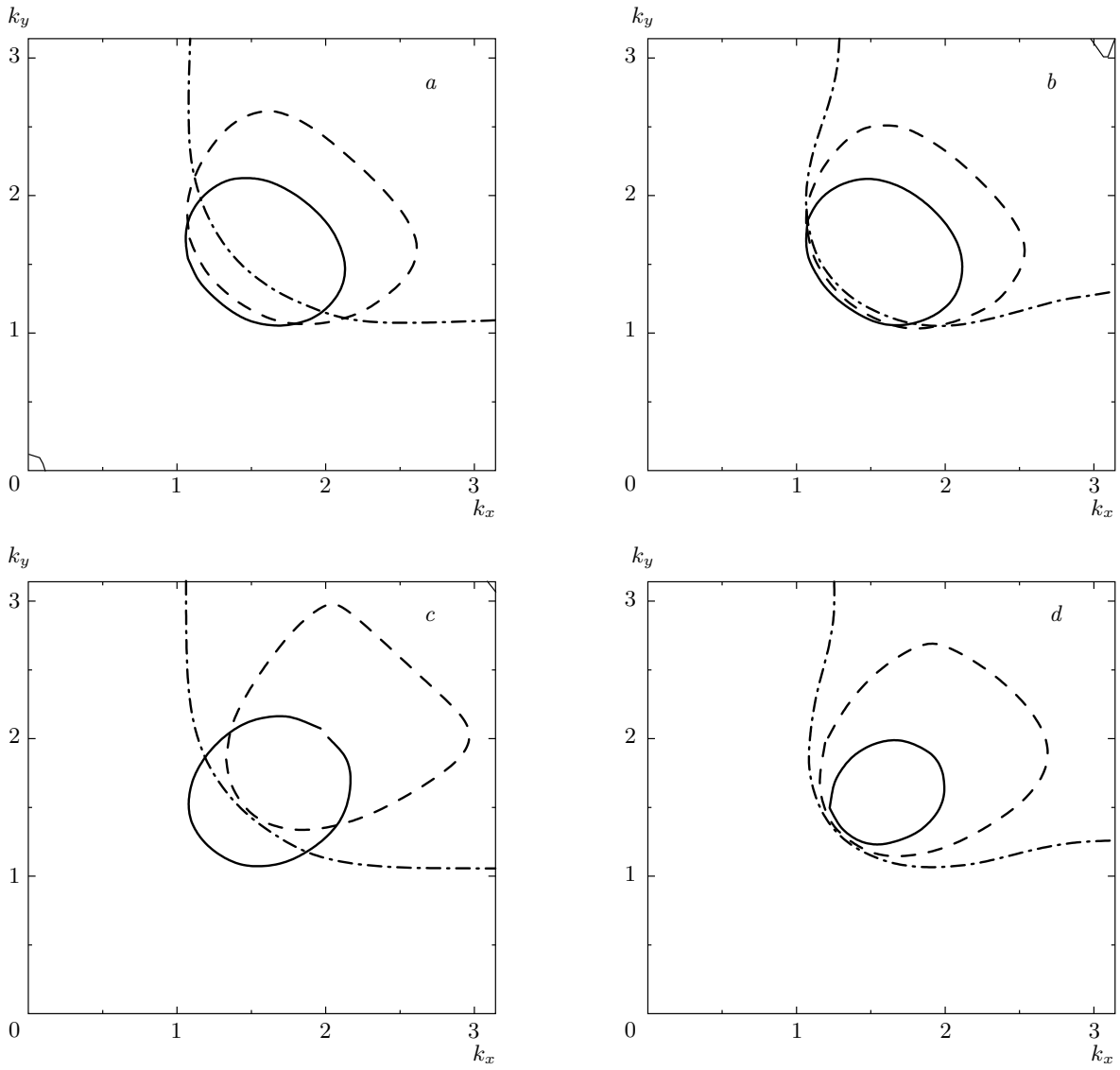

Fig. 2. Fermi surface for (a and c) $V = 0$ and (b and d) $V = 2$ at (a and b) $U = 8$ and (c and d) $U = 16$ in the quarter of the BZ in the GMFA at the hole doping $\delta = 0.05$ (solid line), $\delta = 0.10$ (dashed line), and $\delta = 0.25$ (dash-dotted line)

$(\pm\pi/2, \pm\pi/2)$ points emerge at this doping, as shown in Fig. 2. With increasing doping, the AF correlation length decreases, which results in an increase in the electron energy at the $M(\pi, \pi)$ point, and a large Fermi surface appears at some critical doping $\delta \sim 0.12$. At the same time, the renormalized two-hole subband width increases with doping, for example, for $U = 8$ and $V = 0$, from $\widetilde{W} \approx 2t$ at $\delta = 0.05$ to $\widetilde{W} \approx 3t$ at $\delta = 0.25$, which, however, remains less than the "bare" Hubbard subband width $W = 4t\,(1 + \delta)$ where short-range AF correlations are disregarded. With increasing the CI U and V, the subband width shrinks, as can be seen from the comparison of panels a and b for electronic spectra in Fig. 1 and the Fermi surfaces in Fig. 2.

To study self-energy effects in the electronic spectrum, the strong-coupling theory should be used as a self-consistent solution of the system of equations for the normal GF (36) and self-energy (37). Because the detailed investigation of the normal state electronic spectrum in the strong-coupling theory was performed for the conventional Hubbard model in Ref. [22] and for the extended Hubbard model in Ref. [18], we here present results only for the U and V dependence of the renormalization parameter $Z(\mathbf{q})$ at the Fermi energy,

$$Z(\mathbf{q}) = Z(\mathbf{q},\omega=0) = 1+\lambda(\mathbf{q}) = \\ = 1-[d\,\mathrm{Re}\,\Sigma(\mathbf{q},\omega)/d\omega]|_{\omega=0}. \quad (48)$$

We found that $Z(\mathbf{q})$ weakly depends on δ for $\delta \lesssim 0.15$ (also see Ref. [18]). Therefore, in Fig. 3, we demonstrate the U dependence of $Z(\mathbf{q})$ at $\delta = 0.10$ for $V = 0$ and $V = 1$. It appears that the renormalization parameter $Z(\mathbf{q})$ is quite large in the whole BZ, $Z(\mathbf{q}) \sim$ 4–6, which results in a strong suppression of the quasiparticle weight proportional to $1/Z(\mathbf{q})$.

4.2. Superconducting T_c

For a comparison of various contributions to superconducting gap equation (39), we approximate interaction function (40) by its value close to the Fermi energy. As a result, the static susceptibility $\chi(\mathbf{q}) = \mathrm{Re}\,\chi(\mathbf{q},\omega=0)$ appears in the gap equation instead of dynamical susceptibility (41), (42). It brings us to a BCS-type equation for gap function (39) at the Fermi energy $\varphi(\mathbf{k}) = \varphi(\mathbf{k},\omega=0)$:

$$\varphi(\mathbf{k}) = \frac{1}{N}\sum_{\mathbf{q}} \frac{[1-b(\mathbf{q})]^2\varphi(\mathbf{q})}{[Z(\mathbf{q})]^2 2\widetilde{\varepsilon}(\mathbf{q})}\,\mathrm{th}\,\frac{\widetilde{\varepsilon}(\mathbf{q})}{2T_c}\big\{J(\mathbf{k}-\mathbf{q}) - \\ - V(\mathbf{k}-\mathbf{q}) + \big[(1/4)|t(\mathbf{q})|^2 + |V(\mathbf{k}-\mathbf{q})|^2\big]\chi_{cf}(\mathbf{k}-\mathbf{q}) - \\ - |t(\mathbf{q})|^2\chi_{sf}(\mathbf{k}-\mathbf{q})\theta(\omega_s - |\widetilde{\varepsilon}(\mathbf{q})|)\big\}, \quad (49)$$

where $\widetilde{\varepsilon}(\mathbf{q}) = \varepsilon_2(\mathbf{q})/Z(\mathbf{q})$ is the renormalized energy. Although there are no retardation effects for the exchange interaction and CI and the pairing occurs for all electrons in the two-particle subband, the spin-fluctuation contributions are restricted to the range of energies $\pm\omega_s$ near the Fermi surface, as determined by the θ-function.

To estimate various contributions to gap equation (49), we consider the model d-wave gap function $\varphi(\mathbf{k}) = (\Delta/2)\eta(\mathbf{k})$, where $\eta(\mathbf{k}) = \cos k_x - \cos k_y$. Then the gap equation can be written in the form (see Ref. [18] for the details):

$$1 = \frac{1}{N}\sum_{\mathbf{q}} \frac{[1-b(\mathbf{q})]^2[\eta(\mathbf{q})]^2}{[Z(\mathbf{q})]^2 2\widetilde{\varepsilon}(\mathbf{q})}\,\mathrm{th}\,\frac{\widetilde{\varepsilon}(\mathbf{q})}{2T_c}\big\{J - V + \widehat{V}_{cf} + \\ + (1/4)\,|t(\mathbf{q})|^2\widehat{\chi}_{cf} - |t(\mathbf{q})|^2\,\widehat{\chi}_{sf}\theta(\omega_s - |\widetilde{\varepsilon}(\mathbf{q})|)\big\}. \quad (50)$$

In this equation, only $l = 2$ components of the static susceptibility and the CI give contributions,

Table. Charge-fluctuation contribution $\widehat{V}_{cf}/t$ for several values of the on-site CI U and the intersite CI V for the hole concentration $\delta = 0.10$

U	$V=1$	$V=2$	$V=3$
8	0.10	0.29	0.53
16	0.24	0.76	1.95
32	0.43	1.47	1.71

$$\widehat{V}_{cf} = \frac{1}{N}\sum_{\mathbf{k}} |V(\mathbf{k})|^2\chi_{cf}(\mathbf{k})\cos k_x, \quad (51)$$

$$\widehat{\chi}_{cf} = \frac{1}{N}\sum_{\mathbf{k}} \chi_{cf}(\mathbf{k})\cos k_x, \quad (52)$$

$$\widehat{\chi}_{sf} = \frac{1}{N}\sum_{\mathbf{k}} \chi_{sf}(\mathbf{k})\cos k_x. \quad (53)$$

The contribution from the charge fluctuations $\widehat{\chi}_{cf}$ in (52) weakly depends on U and V and is very small: $\widehat{\chi}_{cf} \sim 10^{-3}(1/t)$–$10^{-2}(1/t)$ for hole concentrations $\delta = 0.05$–0.10. For the vertex $\overline{|t(\mathbf{q})|^2} = (1/N)\sum_{\mathbf{q}}|t(\mathbf{q})|^2 \approx 4t^2$ averaged over the BZ, the contribution induced by the kinematic interaction is equal to $\overline{|t(\mathbf{q})|^2}\,\widehat{\chi}_{cf} \lesssim 0.04t$ and can be neglected. The charge fluctuation contribution $\widehat{V}_{cf}$ in (51) from the intersite CI, Eq. (43), for the hole concentration $\delta = 0.05$ is also small, $\widehat{V}_{cf} \lesssim 5\cdot 10^{-2}t$ for $V \le 2$ and increases to $0.17t$ for $V = 4$. For larger hole concentrations, $\widehat{V}_{cf}$ increases as shown in Table for $\delta = 0.10$. However, $\widehat{V}_{cf} - V < 0$ for all values of U and V, and hence the d-wave pairing induced only by charge fluctuations cannot occur.

The spin-fluctuation contribution $\widehat{\chi}_{sf}$ in (53) is calculated for the model $\chi_{sf}(\mathbf{q})$ in Eq. (46). Since the spin susceptibility has a maximum at the AF wave vector $\mathbf{Q} = (\pi,\pi)$, the integral over $\mathbf{k}$ in (53) results in a negative value of $\widehat{\chi}_{sf}$ that strongly depends on the hole doping. Our previous calculations gave the values $-\widehat{\chi}_{sf}\cdot t \approx 1.3$, 1.0, 0.6 for the respective hole concentrations $\delta = 0.05$, 0.10, 0.25 (see Ref. [18]). Using the vertex $\overline{|t(\mathbf{q})|^2} \approx 4t^2$ averaged over the BZ, we can estimate the effective spin-fluctuation coupling constant as $g_{sf} \approx -4t^2\widehat{\chi}_{sf} = 5.2$, 4.0, 2.4. Thus, the spin-fluctuation contribution to the pairing in Eq. (50) with the coupling constant $g_{sf} = 2$–1 eV for $\delta = 0.05$–0.25 appears to be the largest.

The results of calculating T_c with Eq. (50) are shown in Fig. 4 for $U = 8$, 16 and $V = 0$, 0.5, 1.0, 2.0. A similar doping dependence for T_c is observed for $U = 32$. The maximum T_c at the optimal doping as

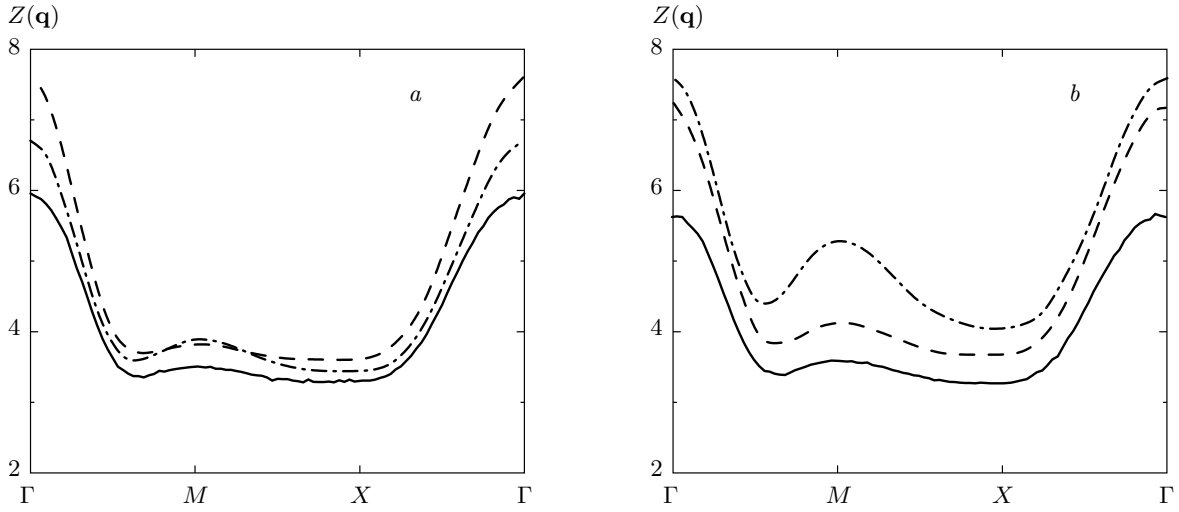

Fig. 3. The renormalization parameter $Z(\mathbf{q})$ along the symmetry directions $\Gamma(0,0) \to M(\pi,\pi) \to X(\pi,0) \to \Gamma(0,0)$ at $\delta = 0.10$ at $U = 8$ (solid line), $U = 16$ (dashed line), and $U = 32$ (dash-dotted line) for (a) $V = 0$ and (b) $V = 1$

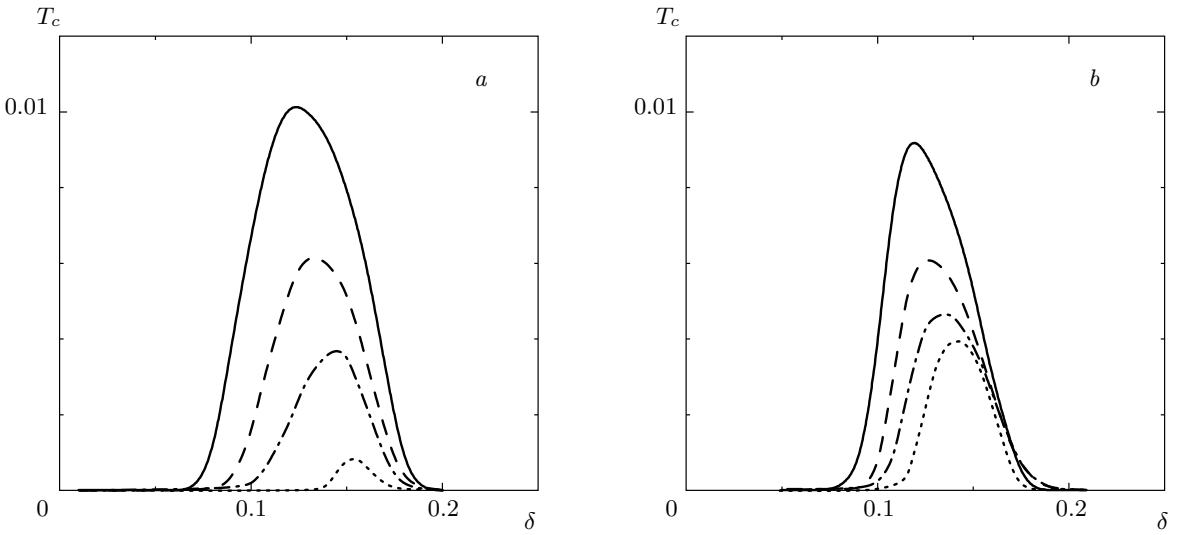

Fig. 4. $T_c(\delta)$ for (a) $U = 8$ and (b) $U = 16$ with $V = 0$ (solid line), $V = 0.5$ (dashed line), $V = 1.0$ (dash-dotted line), and $V = 2.0$ (dotted line)

a function of U and V is shown in Fig. 5. Increasing the intersite Coulomb repulsion V suppresses T_c, which becomes small only for high values $V = 2t$–$3t$ comparable with the spin-fluctuation coupling g_{sf} and much larger than the exchange interaction $J = 0.4t$. At the same time, increasing U enhances T_c. This is due to the narrowing of the electronic band as seen in Fig. 1 and the corresponding increase in the density of state.

To prove an important role of the spin-fluctuation interaction both in the normal state and in superconducting pairing, we calculate the function $Z(\mathbf{q})$ in (48) and T_c for several values of the parameter ω_s for the static susceptibility in model (46): $\omega_s = 0.2$, 0.4, 0.6, 1.0 for $U = 8$. Figure 6 shows the T_c dependence on the parameter ω_s that determines the spin-fluctuation contribution $\widehat{\chi}_{sf}$ in Eq. (50) in two cases: for $Z(\mathbf{q})$ given by Eq. (48) and $Z(\mathbf{q}) = 1$. Because the spin-fluctuation interaction is determined by $\chi_Q \propto 1/\omega_s$ in (47), it

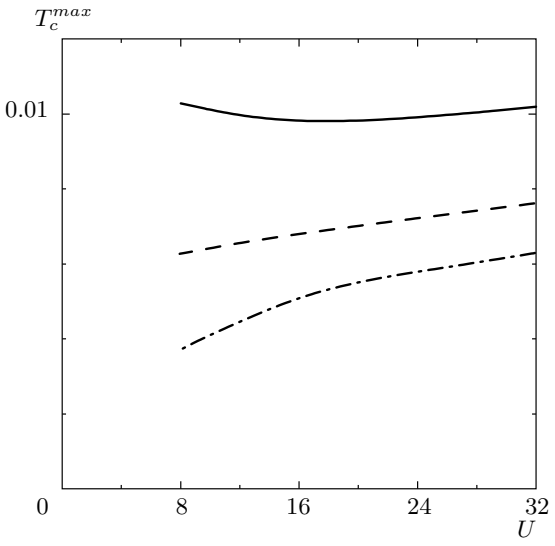

Fig. 5. Maximum $T_c(\delta)$ as a function of U for $V = 0$ (solid line), $V = 0.5$ (dashed line), and $V = 1.0$ (dash-dotted line)

increases as the cut-off frequency ω_s decreases. This results in an increase in the superconducting pairing contribution $\widehat{\chi}_{sf}$, but at the same time enhances the normal state renormalization $Z(\mathbf{q})$ as shown in Fig. 7. Therefore, in case for $Z(\mathbf{q})$ given by Eq. (48), T_c, being roughly proportional to $\widehat{\chi}_{sf}/Z^2(\mathbf{q})$, decreases due to suppression of the quasiparticle weight $1/Z(\mathbf{q})$, while in case for $Z(\mathbf{q}) = 1$, increasing the pairing strength results in a T_c increase. We also note that T_c in Fig. 6*b* calculated in the mean-field approximation (MFA) with $Z(\mathbf{q}) = 1$ is an order of magnitude larger than its value with a proper consideration of the electronic spectrum renormalization.

In the current approach, we can also consider the s-wave pairing. For the extended s-wave gap function $\varphi_s(\mathbf{k}) = (\Delta/2)\eta_s(\mathbf{k})$, where $\eta_s(\mathbf{k}) = \cos k_x + \cos k_y$, an equation for T_c similar to (49) can be derived. Solving this equation reveals a finite and quite high T_c. However, s-wave pairing symmetry violates the kinematic restriction of no double occupancy for the Hubbard model in the two-subband regime. As was pointed out in Refs. [27, 28], the single-site correlation function should obey the condition

$$\langle X_i^{\bar{\sigma}2} X_i^{\sigma 2}\rangle = \frac{1}{N}\sum_{\mathbf{q}} \langle X_{-\mathbf{q}}^{\bar{\sigma}2} X_{\mathbf{q}}^{\sigma 2}\rangle = 0, \qquad (54)$$

caused by the multiplication rule for the Hubbard operators, $X_i^{\alpha\beta} X_i^{\gamma\delta} = \delta_{\beta\gamma} X_i^{\alpha\delta}$. In the quasiparticle approximation used in Eq. (49), we obtain the relation

$$\langle X_i^{\bar{\sigma}2} X_i^{\sigma 2}\rangle = \frac{1}{N}\sum_{\mathbf{q}} \frac{\varphi(\mathbf{q})}{[Z(\mathbf{q})]^2 2\widetilde{\varepsilon}(\mathbf{q})} \operatorname{th}\frac{\widetilde{\varepsilon}(\mathbf{q})}{2T_c} = 0. \qquad (55)$$

For the d-wave pairing $\varphi_d(\mathbf{q}) = (\Delta/2)(\cos q_x - \cos q_y)$, this condition is fulfilled in the tetragonal phase for any doping (pairing in the orthorhombic pase is considered in Ref. [29]). For the s-wave pairing, this condition is violated,

$$\frac{1}{N}\sum_{q_x, q_y} \frac{\cos q_x}{[Z(\mathbf{q})]^2 2\widetilde{\varepsilon}(\mathbf{q})} \operatorname{th}\frac{\widetilde{\varepsilon}(\mathbf{q})}{2T} \neq 0, \qquad (56)$$

for an arbitrary doping except a particular choice of the chemical potential such that the contribution from the integral over $0 \leq q_x \leq \pi$ is compensated by the integral over $\pi \leq q_x \leq 2\pi$. The same condition holds for the one-particle subband, $\langle X_i^{0\bar{\sigma}} X_i^{0\sigma}\rangle = 0$. The obtained results can be derived for the general representation of the correlation function

$$\langle X_{-\mathbf{q}}^{\bar{\sigma}2} X_{\mathbf{q}}^{\sigma 2}\rangle = -\frac{1}{\pi Q_2 N} \times \\ \times \sum_{\mathbf{q}} \int_{-\infty}^{\infty} \frac{dz}{e^{z/T}+1} \operatorname{Im} F_\sigma^{22}(\mathbf{q}, z),$$

since the symmetry of the anomalous GF $F_\sigma^{22}(\mathbf{q}, z)$ is determined by the s- or d-wave symmetry of the gap function. Therefore, we conclude that s-wave pairing is prohibited for the Hubbard model in the limit of strong correlations.

4.3. Comparison with previous theoretical studies

As discussed in Sec. 1, the intersite Coulomb repulsion V is detrimental to the pairing induced by the on-site CI U in the Hubbard model or higher-order contributions from V in the weak correlation limit. Here, we comment on several studies of this problem in the strong correlation limit and compare them with our analytic results for the d-wave pairing.

Following the original idea of Anderson [3], it is commonly believed that the exchange interaction $J = 4t^2/U$ induced by the interband hopping in the Hubbard model plays a major role in the d-wave superconducting pairing. Because the excitation energy of electrons in the interband hopping U is much larger than their intraband kinetic energy W, the exchange pairing has no retardation effects, contrary to the case of electron–phonon pairing, where a large Bogoliubov–Tolmachev logarithm [30] diminishes the Coulomb repulsion as $V \to V/[1 + \rho_c \ln(\mu/\omega_{ph})]$, where

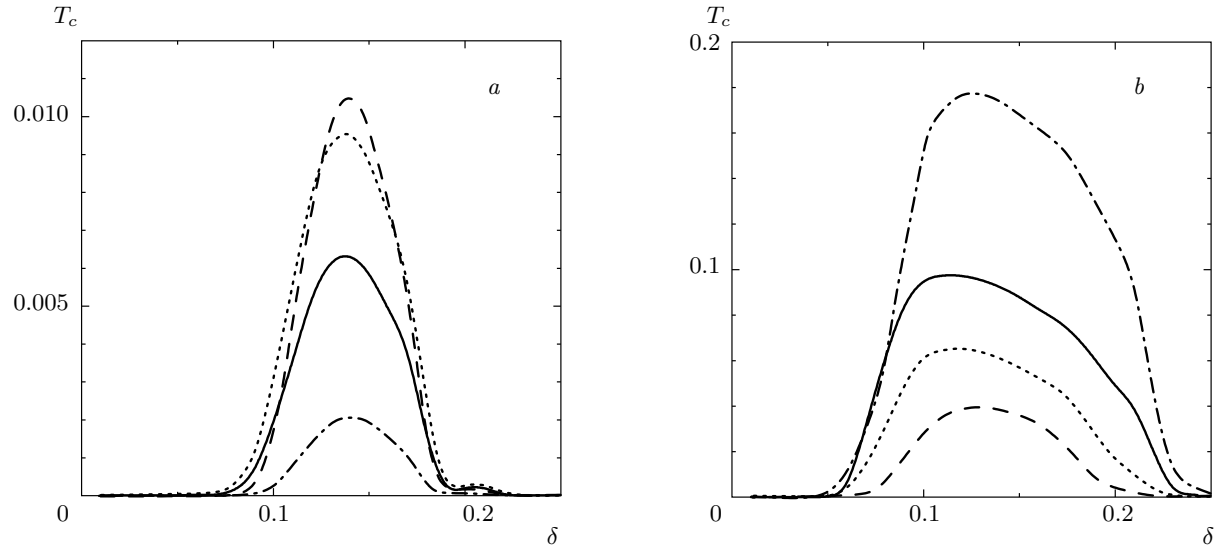

Fig. 6. $T_c(\delta)$ dependence on the spin-fluctuation contribution $\hat{\chi}_{sf}$ in Eq. (50) for $\omega_s = 0.2$ (dash-dotted line), $\omega_s = 0.4$ (solid line), $\omega_s = 0.6$ (dotted line), and $\omega_s = 1.0$ (dashed line) calculated for (a) finite $Z(\mathbf{q})$ and (b) $Z(\mathbf{q}) = 1$

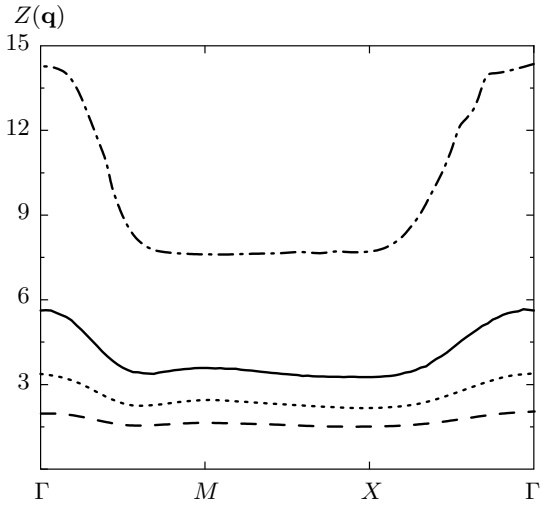

Fig. 7. $Z(\mathbf{q})$ dependence on spin-fluctuation contribution $\hat{\chi}_{sf}$ in Eq. (48) for $\omega_s = 0.2$ (dash-dotted line), $\omega_s = 0.4$ (solid line), $\omega_s = 0.6$ (dotted line), and $\omega_s = 1.0$ (dashed line) at $\delta = 0.10$

$\rho_c = N(0)\,V$ and ω_{ph} is the phonon energy. Consequently, without the retardation effects, the Coulomb repulsion V should destroy the exchange pairing for $V > J$.

To overcome this problem, it was suggested in Ref. [16] that in the limit of strong correlations, the intersite Coulomb repulsion V decreases the interband excitation energy, which results in an enhancement of the exchange interaction, $\widetilde{J}(V) = 4t^2/(U - V)$, as was found from cluster calculations. If we consider the pairing induced only by the exchange interaction $\widetilde{J}(V)$ and take the Coulomb repulsion V into account, then the condition $\widetilde{J}(V) - V > 0$ should be fulfilled for the existence of pairing. The condition is satisfied for $0 < V < V_1$, where $V_1 = (U/2)[1 - \sqrt{1 - (4t/U)^2}]$ for $0 \leq V < U$. For $U > 4t$, we have $V_1 \ll U$, e. g., $V_1 = 0.067U$ for $U = 8$ and $V_1 = 0.004U$ for $U = 32$. Therefore, we see that the pure exchange superconducting pairing can occur in the region of weak Coulomb repulsion. Contrary to this, in Ref. [16], using the cellular dynamical mean-field theory (CDMFT) [14], the d-wave pairing was found in the strong-coupling region up to $V \lesssim U/2$ (e. g., as shown in Fig. 3, $V \leqslant 3t(8t)$ for $U = 8t(16t)$, respectively). At the same time, in the limit of weak correlations $U = 4t$, the pairing is suppressed at the smaller value $V \approx 1.5t$. Thus, we believe that the "resilience of d-wave superconductivity to nearest-neighbor repulsion" is not due to the renormalization of the exchange interaction $\widetilde{J}(V)$ but due to another mechanism of pairing not explicitly seen in CDMFT calculations. As we have shown, in the strong correlation limit, the emerging kinematic interaction in the two-subband regime is responsible for the spin-fluctuation pairing at large values of V, up to $V \lesssim 4t$.

Our conclusion about the importance of the kinematic mechanism of pairing is supported by the studies in Ref. [15]. Using the variational Monte Carlo technique, the superconducting d-wave gap was calculated

for the extended Hubbard model with the weak exchange interaction $J = 0.2t$ and a repulsion $V \leq 3t$ in the wide range $0 \leq U \leq 32$. It was found that the gap decreases with increasing V at all U and can be suppressed for $V > J$ for small U. But for large $U \gtrsim U_c \sim 6t$, the gap becomes robust and exists up to large values $V \sim 10J = 2t$, which was explained by an effective enhancement of J as in Ref. [16]. At the same time, the gap does not show notable variation with U for large $U = 10$–30, although it should depend on the conventional exchange interaction in the Hubbard model as $J = 4t^2/U$ (or $J = 4t^2/(U - V)$). We can suggest another explanation of these results by pointing out that at large $U \gtrsim U_c$, concomitant decrease of the bandwidth (as shown in Fig. 3*b* in Ref. [15]) results in the splitting of the Hubbard band into the upper and lower subbands and the emerging kinematic interaction induces the d-wave pairing in one Hubbard subband. In that case, the second subband gives a small contribution for large U, which results in a U-independent pairing. It can be suppressed only by the repulsion V larger than the kinematic interaction, $V \gtrsim 4t$.

In Ref. [17], the extended Hubbard model is considered in the weak or intermediate correlation limits as in Ref. [6] and in the strong correlation limit within the slave-boson representation in the MFA. In the strong correlation limit, the small value $V = J$ was found, which suppresses the d-wave superconducting gap. However, in the MFA, the kinetic energy term described by the projected electron operators,

$$t\hat{c}^{\dagger}_{i\sigma}\hat{c}_{j\sigma} = tc^{\dagger}_{i\sigma}(1 - n_{i-\sigma})c_{j\sigma}(1 - n_{j-\sigma}) \equiv tX^{\sigma 0}_{i}X^{0\sigma}_{j}$$

is approximated by the conventional fermion (spinon) operators $t\delta f^{\dagger}_{i\sigma}f_{j\sigma}$, and the most important contribution from the kinematic interaction is lost in the resulting BCS-type gap equation (13) in Ref. [17]. As shown in our equation for the gap, Eq. (50), the kinematic interaction given by $\widehat{\chi}_{sf}$ in (53) provides strong spin-fluctuation pairing and high T_c.

To analyze the pairing mechanisms in the limit of strong correlations, analytic methods should be used. A complicated dynamics of projected electron operators can be rigorously taken into account using the HO technique. The algebra of the HOs rigorously preserves the restriction of no double occupancy of quantum states, which is violated in the commonly used MFA in the slave-particle theory. As discussed in Sec. 2.1, the commutation relations for the HOs result in a kinematic interaction that is responsible for the strong spin-fluctuation electron interaction. The superconducting pairing induced by the kinematic interaction for the HOs was first proposed by Zaitsev and Ivanov [31], who studied the two-particle vertex equation by applying the diagram technique for HOs. The momentum-independent s-wave superconducting gap was found, which, however, violates the HO kinematics, as was shown in Refs. [27, 28]. Because the intersite Coulomb repulsion $V > J$ destroys the superconductivity induced by the AF exchange interaction, the spin-fluctuation pairing in the second order of the kinematic interaction beyond the GMFA should be taken into account as discussed in detail in Sec. 4.2 and considered in Refs. [32, 33] for the t–J model.

5. CONCLUSION

We have studied effects of the strong intersite Coulomb repulsion V on the d-wave superconducting pairing within the extended Hubbard model (1) in the limit of strong electron correlations, $U \gg t$. Using the Mori-type projection technique, we obtained a self-consistent system of equations for normal and anomalous (pair) GFs and for the self-energy calculated in the SCBA.

It was found that the kinematic spin-fluctuation interaction g_{sf} induced by electron hopping in one Hubbard subband is much stronger than the conventional exchange interaction J resulting from the interband hopping. Consequently, the d-wave pairing can be suppressed only for large values $V > g_{sf}$ where g_{sf} is of the order of the kinetic energy, $g_{sf} \sim W \approx 4t$. Since in cuprates, the Coulomb repulsion V is of the same order as the exchange interaction, $V \gtrsim J \sim 0.4t$, and therefore the kinematic spin-fluctuation pairing mechanism plays the major role in achieving HTSC. It is also shown that the kinematic spin-fluctuation interaction results in a strong renormalization of the electronic spectra.

It is important to note that the superconducting pairing induced by the AF exchange interaction and the spin-fluctuation kinematic interaction is characteristic of systems with strong electron correlations. These mechanisms of superconducting pairing are absent in the fermionic models and are generic for cuprates. Therefore, we believe that the spin-fluctuation kinematic mechanism of superconducting pairing in the Hubbard model in the limit of strong correlations is the relevant mechanism of HTSC in copper-oxide materials.

The authors thank A. S. Alexandrov, V. V. Kabanov, A.-M. S. Tremblay, and M. Yu. Kagan for the valuable discussions. Partial financial support by the Heisenberg–Landau Program of JINR is acknowledged.

REFERENCES

1. *Handbook of High-Temperature Superconductivity, Theory and Experiment*, ed. by J. R. Schrieffer and J. S. Brooks, Springer-Verlag, New York (2007).
2. N. M. Plakida, *High-Temperature Cuprate Superconductors*, Springer Ser. in Solid-State Sci., Vol. 166, Springer-Verlag, Berlin (2010), Ch. 7.
3. P. W. Anderson, Science **235**, 1196 (1987); *The Theory of Superconductivity in the High-T_c Cuprates*, Princeton Univ. Press, Princeton (1997).
4. J. Hubbard, Proc. Roy. Soc. London A **276**, 238 (1963).
5. A. S. Alexandrov and V. V. Kabanov, Phys. Rev. Lett. **106**, 136403 (2011).
6. S. Raghu, E. Berg, A. V. Chubukov, and S. A. Kivelson, Phys. Rev. B **85**, 024516 (2012).
7. W. Kohn and J. M. Luttinger, Phys. Rev. Lett. **15**, 524 (1965).
8. M. Yu. Kagan, D. V. Efremov, M. S. Marienko, and V. S. Val'kov, Pis'ma v Zh. Eksp. Teor. Fiz. **93** 725 (2011).
9. D. V. Efremov, M. S. Marenko, M. A. Baranov, and M. Yu. Kagan, Zh. Eksp. Teor. Fiz. **117**, 990 (2000).
10. M. Yu. Kagan, V. V. Val'kov, V. A. Mitskan, and M. M. Korovushkin, Zh. Eksp. Teor. Fiz. **144**, 837 (2013).
11. E. Dagotto, Rev. Mod. Phys. **66**, 763 (1994).
12. N. Bulut, Adv. in Phys. **51**, 1587 (2002).
13. D. J. Scalapino, in Ref. [1], p. 495.
14. D. Sénéchal, in *Theoretical Methods for Strongly Correlated Systems*, ed. by A. Avella and F. Mancini, Springer Ser. in Solid-State Sciences, Vol. 171, Springer-Verlag, Berlin (2012), Ch. 11.
15. E. Plekhanov, S. Sorella, and M. Fabrizio, Phys. Rev. Lett. **90**, 187004 (2003).
16. D. Sénéchal, A. Day, V. Bouliane, and A.-M. S. Tremblay, arXiv:1212.4503.
17. S. Raghu, R. Thomale, and T. H. Geballe, Phys. Rev. B **86**, 094506 (2012).
18. N. M. Plakida and V. S. Oudovenko, Eur. Phys. J. B **86**, 115 (2013).
19. J. Hubbard, Proc. Roy. Soc. London A **285**, 542 (1965).
20. H. Mori, Progr. Theor. Phys. **34**, 399 (1965).
21. D. N. Zubarev, Usp. Fiz. Nauk **71**, 71 (1960); *Nonequilibrium Statical Thermodynamics*, Consultant Bureau, New York (1974).
22. N. M. Plakida and V. S. Oudovenko, Zh. Eksp. Teor. Fiz. **131**, 259 (2007).
23. N. M. Plakida, L. Anton, S. Adam, and Gh. Adam, Zh. Eksp. Teor. Fiz. **124**, 367 (2003).
24. G. M. Eliashberg, Zh. Eksp. Teor. Fiz. **38**, 966 (1960); **39**, 1437 (1960).
25. A. A. Vladimirov, D. Ihle, and N. M. Plakida, Phys. Rev. B **80**, 104425 (2009).
26. J. Jaklič and P. Prelovšek, Phys. Rev. Lett. **74**, 3411 (1995); **75**, 1340 (1995).
27. N. M. Plakida, V. Yu. Yushankhai, and I. V. Stasyuk, Physica C **160**, 80 (1989).
28. V. Yu. Yushankhai, N. M. Plakida, and P. Kalinay, Physica C **174**, 401 (1991).
29. N. M. Plakida and V. S. Oudovenko, Physica C **341–348**, 289 (2000); in *Proc. of the NATO ARW on Open Problems in Strongly Correlated Systems*, ed. by J. Bonca, P. Prelovsek, A. Ramsak, and S. Sarkar, Kluewer Acad. Publ., Dordrecht (2001), p. 111.
30. N. N. Bogoliubov, V. V. Tolmachev, and D. V. Shirkov, *New Method in the Theory of Superconductivity*, Publ. Dept. USSR Acad. of Science, Moscow, (1958); Consultants Bureau, Chapman and Hall, New York–London (1959), Vol. YII.
31. Р. О. Зайцев, В. А. Иванов, ФТТ **29**, 2554 (1987); **29**, 3111 (1987); Int. J. Mod. Phys. B **5**, 153 (1988).
32. N. M. Plakida and V. S. Oudovenko, Phys. Rev. B **59**, 11949 (1999).
33. P. Prelovšek and A. Ramšak, Phys. Rev. B **72**, 012510 (2005).